Impact of fabrication process of polyethylene / boronnitride nanocomposite on morphology and dielectric properties

C. Villeneuve-Faure, N. Lahoud Dignat, B. Lantin, R. Arinero, M. Ramonda, M. Semsarilar, M. Bechelany, Séverine Le Roy, J. Castellon

Impact of fabrication process of polyethylene / boron-nitride nanocomposite on morphology and dielectric properties

C. Villeneuve-Faure[1], N. Lahoud Dignat[1], B. Lantin[1], R. Arinero[2], M. Ramonda[2], M. Semsarilar[3], M. Bechelany[3], S. Le Roy[1], J. Castellon[2]
[1] LAPLACE, Université de Toulouse, CNRS, INPT, UPS, Toulouse, France,
[2] IES, Université de Montpellier, Montpellier, France
[3] IEM –UMR 5635, Univ Montpellier, ENSCM, CNRS, Montpellier, France

***Abstract*- Nanocomposite (NC) films are extensively investigated due to their improved properties attributed to the interphase formed between the nanoparticle and the matrix. In this work, we focus our interest on Polyethylene (PE) / Boron Nitride (BN) NC. The objective of this paper is to investigate the influence of BN concentration and film thickness on NC morphology and interphase properties. Scanning Electron Microscopy (SEM), Atomic Force Microscopy (AFM) and its derived mode the Electrostatic Force Microscopy (EFM) are used to characterize the NC morphology and relative dielectric permittivity (ε_r). Results show that an increase of the BN concentration has no influence on the crystallinity degree even if a disappearance of spherulite structures is observed. An increase of the surface roughness is observed as well and is more pronounced for thicker NC films. Moreover, it is shown that the interphase ε_r is lower than the matrix one and the BN concentration seems to have no influence on neither the interphase thickness nor its ε_r.**

I. INTRODUCTION

Polymer-based nanocomposite (NC) appears as the best way to improve electrical insulation properties for various applications ranging from microelectronic devices to electrical machines and HVDC cables [1-3]. Indeed, results reported in the literature emphasize that the adjunction of a small amount (i.e. few weight percent) of nanoparticles (NP) could increase the breakdown strength and the dielectric permittivity or decrease the leakage current [1, 4-5]. This improvement is attributed to the presence of an interphase area, surrounding the NP, whose properties differ from the matrix and NP ones [6]. According to the literature, the interphase area seems to exhibit a more ordered polymer chains than the matrix [7-8], to have a lower dielectric permittivity [8-9] and deeper traps [10]. However, the interphase properties remain poorly characterized mainly at the nanoscale and the relevant influencing parameters (e.g. NPs shape, dimension, nature, surface treatment or concentration) need to be identified. In addition to the interphase properties, another drawback is related to the control of NP dispersion in the polymer matrix [11]. Indeed, NP aggregation leads to the deterioration of not only electrical properties (breakdown strength, conductivity…), but also mechanical and thermal ones. Finally, the effect of the NC film thickness is rarely investigated even if some papers report an influence on morphology [12] and on deep-trap density [13]. In this context, the present paper deals with the impact of NP elaboration process and concentration on morphological and dielectric properties. To reach this goal, Scanning Electron Microscopy (SEM) and Atomic Force Microscopy (AFM) are used to characterize the morphology. The interphase dielectric properties are addressed using Electrostatic Force Microscopy (EFM), which appears as a promising tool to characterize a nanoscale permittivity [7-9, 14]. For this study, we focus our interest on low density polyethylene (LDPE) / boron nitride (BN) NC. Indeed, LDPE is widely used as insulating material in various applications. LDPE NC presents interesting properties in terms of space charge limitation (LDPE/SiO_2 [10, 13], LDPE/TiO_2 [15], LDPE/ZnO [11]), dielectric strength improvement (LDPE/MgO [16], LDPE/TiO_2 [17] or tree inception voltage increase (LDPE/Al_2O_3 [18]). However, interphase properties in LDPE-based NC have not yet been investigated.

II. MATERIALS AND METHODS

A. Materials processing

Preparation of casting solution. 1.0 gr of PE (Borealis) containing no additives was dissolved in 10 mL of hot toluene and stirred at 80 ° C. 100 mg of BN (Sigma-Aldrich, nanopowder, ⩽ 150 nm avg. size) for a 10 wt.% BN-LDPE and 10 mg of BN for a 1 wt.% BN-LDPE were added to the hot PE in toluene and continued stirring at 80 °C for 3h.

Film preparation. A clean Teflon sheet was placed on a heated (90 °C) doctor blade platform for 1h prior to film casting. For each film 5 mL of the hot casting solution was transferred onto the Teflon sheet at 90 °C and the solution was spread using a blade whose dimension depends on target thickness. For a 6 µm-thick film a 10 or 20 µm blade with speed 1 is used whereas a 400 µm-thick blade with speed 1 is used for 20 µm-thick films. The heating was then switched off, allowing the temperature to drop gradually. The films were then placed in a water bath for 30 minutes, before peeling the PE/BN film off the Teflon support. For preparation of the reference films (pure LDPE), the same procedure was followed using the casting solution with no BN (1.0 gr PE in 10 mL toluene). Silicon wafer supported samples were

prepared via manual dip coating using hot casting solutions at 80 °C. The samples where then dried at ambient conditions.

B. Nano- and macro-scale characterization

The PE/BN NC films morphology was characterized by SEM in cross-section (SEM FEI Hélios nanolab 600i using 2 kV for the acceleration voltage) and AFM in tapping mode (Bruker Multimode 8).

The crystallinity degree was determined by Differential Scanning Calorimetry (DSC) (TA Instruments DSC 2010). Measurements were performed under N2 atmosphere at a flow rate of 40 ml/min and a temperature gradient from -150 °C to 150 °C with a heating rate of 10 °C/min.

The relative dielectric permittivity (ε_r) of the PE/BN NC films was deduced from EFM phase shift $\Delta\Phi$ measurements (Bruker Multimode 8 apparatus). A PtIR-coated silicon tip (resonance frequency f_0 = 63.2 kHz, spring constant k = 6.7 N.m^{-1}, quality factor Q = 355 and curvature radius R_c = 26 nm) and a 50 nm-lift were used. The phase shift $a_{\Delta\Phi}$ parameter is deduced using the following equation [19]:

$$a_{\Delta\Phi} = [\Delta\Phi(V_1) - \Delta\Phi(V_2)]/[V_1^2-V_2^2] \quad (1)$$

where $\Delta\Phi(V_i)$ is the phase shift measured with a bias voltage V_i (respectivelly 0 V and 10 V) applied on the tip whereas the sample backside is grounded.

The methodology developped to extract the ε_r cartography from the measured phase (or frequency) shift parameter is composed of three steps [8]. First, the electric field distribution in air and in the dielectric layer as well as the electrostatic force (F_e) on the AFM-tip were computed using a 2D-axisymmetric finite element model (FEM) on COMSOL Multiphysics®. Secondly, the second derivative of the capacitance between the AFM probe and the sample (d^2C / dz^2) was deduced from F_e. Finaly the related phase shift $a_{\Delta\Phi}$ parameter is computed using:

$$a_{\Delta\Phi} = [Q/(k)]\,[d^2C/dz^2] \quad (2)$$

It is to note that the phase shift parameter $a_{\Delta\Phi}$ can be computed for various configurations, such as an homogeneous material and NC films with or without interphase.

III. RESULTS AND DISCUSSION

A. PE/BN nanocomposite films morphology

Fig. 1.a presents the surface topography of a 6 µm-thick pure LDPE film. Spherulites can be observed, with a radius of around 2 µm. The same morphology is observed for 20 µm-thick pure LDPE films. An arithmetic surface roughness R_a of 30 nm and 36 nm is measured for the 6 µm-thick and the 20 µm-thick LDPE film respectively. A further analysis of the PE morphology using the Power Spectrum Density (PSD) approach is used [20]. The PSD was plotted as a function of frequency for different AFM surface topography scans (inset of Fig. 1.a). At high frequencies (80 µm^{-1} – 300 µm^{-1}), the fractal model can be applied and the PSD can be expressed by:

$$PSD = K/f^s \quad (3)$$

where K is the spectral strength, f the frequency and s the slope of the PSD logarithmic plots vs spatial frequency.

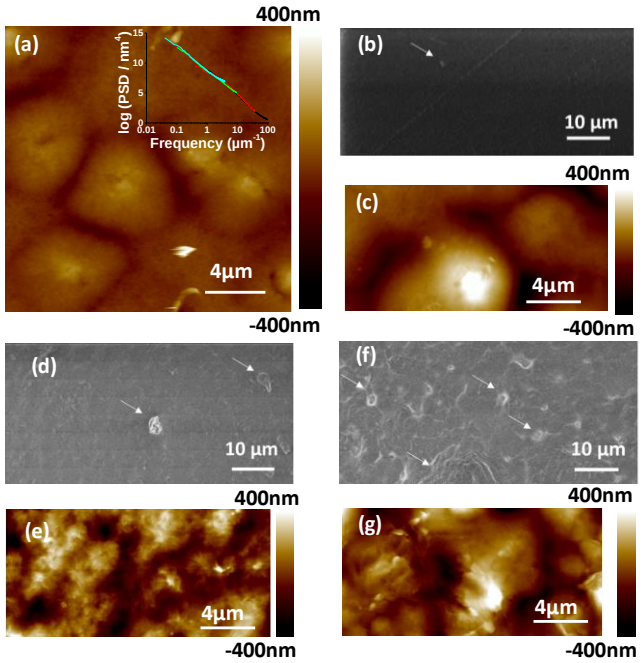

Fig.1. (a) AFM surface topography of 6 µm-thick pure LDPE. Inset the 2D Power Spectrum Density (PSD) for 50 µm x 50 µm (blue), 20 µm x 20 µm (green), 5 µm x 5 µm (red) and 2 µm x 2 µm (black) scans. (b) SEM and (c) AFM surface topography of 20 µm-thick 1 wt.% PE/BN NC. (d, f) SEM and (e, g) AFM surface topography of (d, e) 6 µm-thick and (f, g) 20 µm-thick 10 wt.% PE/BN NC.

At low frequencies (1 µm^{-1} – 30 µm^{-1}), the k-model can be applied and the PSD can be expressed as:

$$PSD = A/(1+B^2f^2)^{C+1/2} \quad (4)$$

where A, B and C are fitting parameters related to the surface morphology. The more important one is B as it corresponds to the correlation length.

For pure LDPE, the slope s is around 1 which implies a fractal dimension D of 2 and an inhomogeneous distribution (i.e. abrupt variation) of peaks over the surface. Moreover, a correlation length B of 12 µm is obtained which is higher than the spherulite lateral dimension (between 4 µm and 6 µm). This is probably related to the fact that spherulites are not observed over the entire surface.

Fig. 1.b and Fig. 1.c compare the surface morphology of 1 wt.% PE/BN probed by SEM and AFM respectively. At large scale (Fig. 1.b) the NC surface seems flat and only one aggregate is observed. At small scale (Fig. 1.c) the NC surface is similar to the pure LDPE one and spherulites are observed.

When the amount of BN NP increases to 10 wt.%, the surface morphology is modified. At large scale, the amount of aggregates increases and this is more pronounced for thicker NC films (Fig. 1.d and 1.f). Moreover, spherulites are no more visible at small scale and the surface morphology appears rough (Fig. 1.e and Fig. 1.g). PSD plots for nanocomposites are similar to pure LDPE ones.

Surface roughness R_a, fractal dimension D and correlation length B are summarized in Table 1. For 1 wt.% PE/BN NC the R_a, and the B are similar to pure PE. However, when the amount of BN NP increases up to 10 wt.% R_a, increases and B decreases.

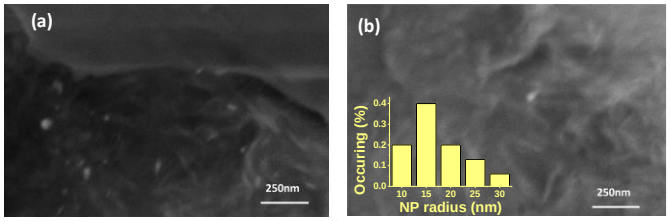

Fig. 2. SEM picture in cross-section of (a) 20 µm-thick 1 wt.% NC and (b) 6 µm-thick 10 wt.%

TABLE I
Surface roughness R_a, fractal dimension D, correlation length B and crystallinity degree χ_c for PE and NC films.

Material	Thickness	Ra (nm)	D	B (µm)	χ_c (%)
PE	6 µm	30	2	12	41.2
	20 µm	36	2	12	41.1
PE/BN 1 wt.%	20 µm	25	2	10	38.8
PE/BN 10 wt.%	6 µm	85	2	6	/
	20 µm	85	2	6	38.2

SEM observations for NC cross-sections demonstrate that BN NP are well dispersed in the volume for 1 wt.% (Fig.2.a) or for 10 wt.% (Fig.2.b) even if aggregates are observed on the surface (Fig. 1.b, 1.d and 1.f). According to SEM cross-section observations, the radius of BN NP can be determined. The resulting data are given in the inset of Fig. 2.b. The NP radius mean value is 17 nm ± 6 nm.

Finally, DSC measurements were performed to extract the materials crystallinity degree (χ_c). χ_c is calculated from the melting peak using the following equation:

$$\chi_c = (\Delta H_m / \Delta H_{100}) \times 100 \quad (5)$$

where ΔH_m is the measured melting heat and ΔH_{100} the theoretical melting heat for 100% crystalline PE = 293 J/g [21]. χ_c was calculated for two heating cycles for each sample and the mean value is presented in the last column of Table I. The BN concentration and the NC film thickness have practically no influence on χ_c (taking into consideration the χ_c relative error > 2.3%). Thus, the spherulites disappearance within the 10 wt.% PE/BN has almost no effect on χ_c. The increase of the film thickness favors the formation of BN NP aggregates without impacting χ_c.

B. PE/BN nanocomposite films dielectric properties

EFM measurements and related calculations performed on pure LDPE (not presented in the present paper) lead to a calculated permittivity of 2.2, whatever the thickness. This is in the range of what is usually measured for LDPE. Fig. 3 summarizes EFM measurements performed on PE/BN NC in term of topography and apparent dielectric permittivity. Concerning the 1 wt.% PE/BN, the topography map emphasizes that isolated NP (addressed by black arrow on Fig. 3.a) are observed and present a lower ε_r than the matrix one (Fig. 3.d). Concerning the 6 µm-thick 10 wt.% PE/BN, the topography map (Fig. 3.b) emphasizes that isolated NP (black arrows) as well as NP aggregates (red arrow) are observed. The NP ε_r in this case is also lower than the matrix one (Fig. 3.e). The same observation is true for 20 µm-thick 10 wt.% PE/BN.

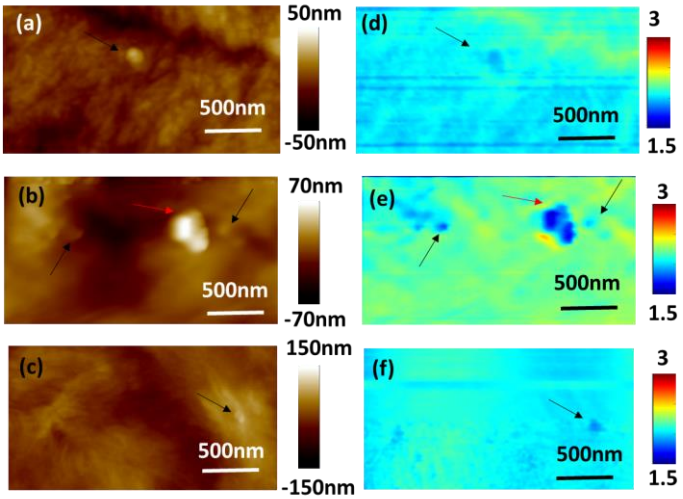

Fig. 3. (a-c) surface topography and (d-f) ε_r maps of (a, d) 20 µm-thick 1 wt.% PE/BN NC, (b, e) 6 µm-thick 10 wt.% PE/BN NC and (c, f) 20 µm-thick 10 wt.% PE/BN NC. Black (red) arrows indicate single NP (aggregate)

For all measured NC, the ε_r far from the NP is calculated in the range from 2 to 2.2, which is close to the LDPE one. Moreover, ε_r over the NP is lower than the matrix one. This phenomenon is inconsistent with the fact that BN presents a higher ε_r than LDPE. This phenomenon has already been observed with EFM measurements on PE/TiO_2 [9] and polyimide/Si_3N_4 [8]) or with dielectric spectroscopy on PE/Al_2O_3 [22]. This permittivity decrease over the NP was attributed to a lower value of the interphase permittivity compared to the matrix one.

Determining the interphase relative permittivity (ε_{ri}) requires to come back to the experimental phase shift parameter $a_{\Delta\Phi}$ results. Fig. 4.a and 4.b compare the topography and $a_{\Delta\Phi}$ profiles over BN NP. Results are shown for a protuberant NP and more particularly for a 50-100 nm-height one. Whatever, the BN NP concentration, $a_{\Delta\Phi}$ is around -0.115±0.005 °/V² over PE and around -0.075±0.005 °/V² over NP.

Moreover a more complex FEM model taking into account the matrix (thickness = 20 µm and ε_r = 2.2), the BN NP (NP radius fixed at 20 nm according to the Fig.2.b inset and ε_r = 4) and the interphase (unknown thickness and ε_{ri}) is needed. Fig. 4.c represents the evolution of the computed phase shift parameter $a_{\Delta\Phi}$ (2) as a function of the interphase ε_{ri} and thickness.

Results highlight that all curves intercept at $a_{\Delta\Phi}$ = -0.1 °/V² and ε_r = 2.2, which corresponds to the PE matrix parameters. Moreover, the $a_{\Delta\Phi}$ variation as a function of ε_{ri} shows a steeper slope for high interphase widths, which implies a higher sensitivity when the interphase width is more important. Moreover, when the interphase ε_{ri} is lower than the matrix one, an increase of the interphase thickness induces an increase of $a_{\Delta\Phi}$ as well. On the contrary when ε_{ri} is higher than the matrix one, an increase of the interphase thickness induces a decrease of $a_{\Delta\Phi}$.

According to Fig. 4.c, a large number of ε_{ri} /thickness couples are possible to describe the interphase for 1 wt.% and 10 wt.% PE/BN. Indeed, the interphase thickness needs to be higher

than 60 nm and its ε_{ri} should be between 1 and 2. These high values for the interphase thickness are consistent with the topography profile width (around 200 nm on Fig 4) and the "shadow" observed around NP aggregates on Fig. 3. Finally, the BN NP concentration seems to have a weak influence on the interphase width and permittivity. This implies that the degradation of NC performances at high NP concentrations (i.e. higher than 2-3 wt.%) observed in a large number of NC [11] should be related to the NP aggregation rather than the interphase thickness.

IV. CONCLUSION

This paper addresses the influence of BN NP concentration and NC film thickness on morphology and dielectric properties. Results highlight that the NC film thickness has a low impact on the crystallinity but favor the NP aggregation. Moreover, an increase of the BN concentration induces the disappearance of the spherulite structure and the surface roughness increase without really affecting the crystallinity degree. Concerning interphase properties, results show that the ε_{ri} is lower than the matrix one and the BN concentration seems to have no influence on neither the interphase thickness nor its dielectric permittivity.

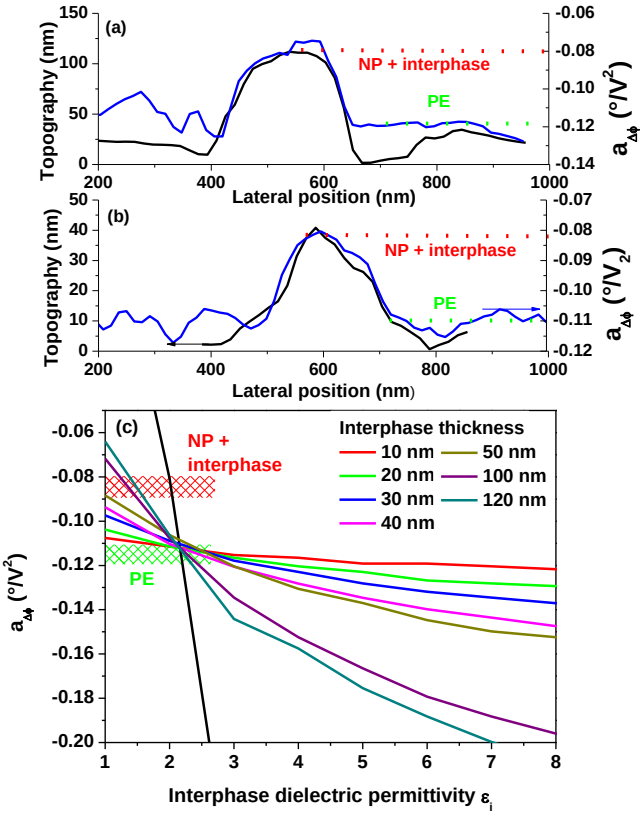

Fig. 4. Topography and phase shitf parameter ($a_{\Delta\Phi}$) profiles over single BN NP for 20 µm-thick (a) 1 wt.% and (b) 10 wt.% PE/BN NC. (c) Evolution of $a_{\Delta\Phi}$ as function of the interphase thickness and permittivity with: NC thickness = 20 µm, BN NP radius = 20 nm and BN ε_r =4)

ACKNOWLEDGMENT

This work was partially funded by CNRS through its energy program (Cellule Energie). This work was partly supported by LAAS-CNRS micro and nanotechnologies platform member of the French RENATECH network.

REFERENCES

[1] J.C. Pandey and M. Singh "Dielectric polymer nanocomposites: past advances and future prospects in electrical insulation perspective" *SPE polymers* Vol.2, pp. 236-256, 2021.
[2] Y.A. Hassan and H. Hu "Current status of polymer nanocomposite dielectric for high-temperature application" *Composites Part. A*, Vol.138, p.106064, 2020.
[3] D.Q. Tan "Review of polymer-based nanodielectric exploration and film scale-up for advances capacitor", *Progress Report* Vol. 30, p. 1808567, 2020.
[4] T. Tanaka, G.C. Montanari, and R. Mulhaupt, "Polymer nanocomposites as dielectrics and electrical insulation-perspectives for processing technologies, material characterization and future applications," *IEEE Trans. Dielectr. Electr. Insul.*, Vol. 11, p.763, 2004.
[5] J.K. Nelson and J. Fothergill "Internal charge behaviour of nanocomposites," *Nanotechnology*, Vol. 15, p.586, 2004.
[6] T.J. Lewis, "Interfaces are the Dominant Feature of Dielectrics at the Nanometric Level," *IEEE Trans. Dielectr. Electr. Insul*., Vol. 11, p.739, 2004.
[7] F. N. Alhabill, R. Ayoob, T. Andritsch and A.S. Vaughan, "Introducing particle interphase model for describing the electrical behaviour of nanodielectrics," *Materials and Design*, Vol. 158, pp.62–73, 2018.
[8] M. Houssat, C. Villeneuve-Faure, N. Lahoud Dignat and J.-P. Cambronne "Nanoscale mechanical and electrical characterization of the interphase in polyimide/silicon nitride nanocomposites" *Nanotechnology* Vol. 32, p.425703, 2021.
[9] S. Peng, Q. Zeng, X. Yang, J. Hu and J. He, "Local dielectric property detection of the interface between nanoparticle and polymer in nanocomposite dielectrics," *Scientific reports*, Vol. 6, p.38978, 2016.
[10] Y. Wang, D. Qiang, Z. Xu, G. Chen and A. Vaughan "The effect of loading ratios and electrical field on charge dynamics in silica-based polyethylene nanocomposites" *J. Phys. D: Appl. Phys*. Vol. 51, 395302, 2018.
[11] H. Luo, *et al.* "Interface design for high energy density polymer nanocomposites", *Chem. Soc. Rev*. Vol. 48, p. 4424, 2019.
[12] J.-G. Gao, X. Li, W.-H. Yang and X.-H. Zhang "Space Charge Characteristics and Electrical Properties of Micro-Nano ZnO/LDPE Composites" *Crystal* Vol. 9, p. 481, 2019.
[13] Z. Lv, X. Wang, K. Wu, X. Chen, Y. Cheng and L. A. Dissado, "Dependence of charge accumulation on sample thickness in Nano-SiO_2 doped IDPE" *IEEE Trans. Dielectr. Electr. Insul*. Vol. 20, p. 337, 2013.
[14] D. El Khoury, R. Arinero, J.-C. Laurentie, M. Bechelany, M. Ramonda and J. Castellon "Electrostatic force microscopy for the accurate characterization of interphases in nanocomposites" *Beilstein J. Nanotechnology* Vol. 9, 2999, 2018.
[15] R. J. Fleming, T. Pawlowski, A. Ammala, P. S. Casey and K. A. Lawrence, "Electrical conductivity and space charge in LDPE containing TiO_2 nanoparticles" *IEEE Trans. Dielectr. Electr. Insul*. Vol. 12, pp. 745-753, 2005
[16] S. Haggag, L. Nasrat and H. Ismail "ANN approaches to determine the dielectric strength improvement of MgO based low density polyethylene nanocomposite" *J. Adv. Dielec.* Vol. 11, p. 2150016, 2021.
[17] D. Ma, T. A. Hugener, R. W. Siegel, A. Christerson, E. Mrtensson, C. Önneby and L. S. Schadler "Influence of nanoparticle surface modification on the electrical behaviour of polyethylene nanocomposites" *Nanotechnology* Vol. 16, p. 724, 2005.
[18] S. Alapati and M. J. Thomas, "Electrical treeing and the associated PD characteristics in LDPE nanocomposites" *IEEE Trans. Dielectr. Electr. Insul*. Vol. 19, pp. 697-704, 2012.
[19] C. Riedel *et al.* "Determination of the nanoscale dielectric constant by means of a double pass method using electrostatic force microscopy" *J. Appl. Phys.* Vol. 106, p.024315, 2009.
[20] Y. Gong, S. T. Misture, P. Gao and N. P. Mellott "Surface Roughness Measurements Using Power Spectrum Density Analysis with Enhanced Spatial Correlation Length" *J. Phys. Chem. C* Vol. 120, p 22358, 2016.
[21] D. Li, L. Zhou, X. Wang, L. He and X. Yang, "Effect of Crystallinity of Polyethylene with Different Densities on Breakdown Strength and Conductance Property" *Materials*, 12(11) 1746, 2019.
[22] S. Wang, P. Chen, S. Yu, P. Zhang, J. Li and S. Li, "Nanoparticle dispersion and distribution in XLPE and the related DC insulation performance" *IEEE Trans. Dielectr. Electr. Insul*. Vol. 25, p 2349, 2018.